Inorganic Chemistry Research

Article

Synthesis of Symmetrical Phenacyl Benzoate Derivatives *via* Ruthenium Hydride–Catalyzed C–C and sp^2–C–O Bonds Formation under Homogeneous and Heterogeneous Conditions

Majid Moghadam*, Shahram Tangestaninejad, Valiollah Mirkhani, Iraj Mohammadpoor–Baltork, Behjat Barati and Moloud Ghafouri

Department of Chemistry, Catalysis Division, University of Isfahan 81746–73441 Iran

Received: July 21, 2023; Accepted: September 3, 2023

Cite This: *Inorg. Chem. Res.* **2022**, *6*, 182-190. DOI: 10.22036/j10.22036.2023.408109.1147

Abstract: In the present work, the catalytic activity of [RuHCl(CO)(PPh_3)$_3$] in the homogeneous form and also supported on graphene oxide nanosheets in the efficient synthesis of phenacyl benzoate derivatives by the reaction of aldehydes with diethyl 2–(ethoxymethylene)malonate (DEMM) *via* hydrogen transfer is reported. Under the same conditions, alcohols were also reacted with DEMM to provide a set of phenacyl benzoate derivatives in good to excellent yields. In these reactions, C–C and sp^2–C–O bonds were formed by applying the ruthenium catalyst. While the homogeneous catalyst is not recoverable, the heterogeneous counterpart was reused several times without loss of its initial activity.

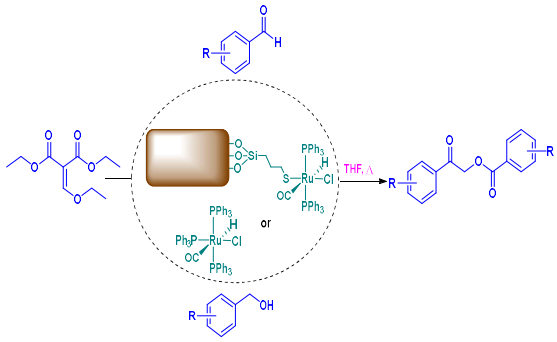

Keywords: Hydrogen transfer, Ruthenium hydride, Homogeneous catalyst, Phenacyl benzoate, Heterogeneous catalyst

1. INTRODUCTION

Construction of chemical bonds, particularly C–C and C–O bonds formation, during the chemical synthesesis a fundamental aspect of synthetic chemistry. A remarkable feature of such constructions may be achieved by metal-catalyzed coupling reactions using rhodium[1], iridium[2-7] or ruthenium catalysts.[8-13] On these grounds, many challenges have been focused on metal–catalyzed C–C bond formation by hydrogen auto–transfer.[14-16] This class of reactions involves initial dehydration of alcohol to an carbonyl intermediate as a nucleophilic reaction precursor. Later, condensation reaction between generated carbonyl electrophile and other reagents delivers a new stable compound which finally undergoes the hydrogenation to give the desired product. The nucleophilic activation of carbonyl electrophile withdiverse unsaturated precursors such as alkynes[8,17,18], enones[19], allenes[11,20], dienes[10,21,22] and enynes[23] has been reported. Construction of C–O bond by transition metal catalysts is also important in organic synthesis[24–26], which less attention has been paid on the using metal–catalyzed hydrogen auto–transfer.

Phenacyl benzoate derivatives are an important class of organic compounds because they have a wide application in organic synthesis. They are used in the preparation of oxazoles, imidazoles and benzoxazepines.[27,28] These compounds are also applied for identification of organic acids and also useful as photo–removable protecting groupsfor carboxylic acids in organic synthesis and biochemistry.[29,30] The most common way for synthesis of phenacyl benzoate derivatives is the reaction of an acid and phenacyl bromide in the presence of a base such as potassium carbonate or triethylamine.[31] Recently, He and co–workers obtained phenacyl benzoate as a by–product in the conversion of styrene to styrene carbonate catalyzed by sodium phosphotungstate/*n*–Bu_4NBr catalytic system.[32]

Graphene is a honeycomb–like two–dimensional nanomaterial composed of sp^2–bonded carbon atoms. It has attracted tremendous attention in recent years due to its unique properties and potential applications.[33-35] The main disadvantage of graphene in catalytic experiments is the lack of functional groups on its surface. The oxidation form of graphene, graphene oxide (GO), contains a wide range of oxygen carrying

functional groups on its basal planes and edges.[36–38] These functional groups can be used for attachment of metal complexes.[39-42]

In continuation of our interest in the application of $[RuHCl(CO)(PPh_3)_3]$ in the organic transformations,[43–46] here, we report a novel approach for the synthesis of symmetrical phenacyl benzoate derivatives based on ruthenium hydride–catalyzed C–C and C–O bond forming via hydrogen transfer. In this regard, our attention was focused on the unique catalytic activity of $[RuHCl(CO)(PPh_3)_3]$ in the reaction of aldehydes or alcohols with diethyl 2–(ethoxymethylene)malonate (DEMM) to achieve this goal (Scheme 1). To the best of our knowledge, this method is the first metal–catalyzed hydrogen auto–transfer reaction for synthesis of phenacyl benzoate derivatives based on C–C and sp^2–C–O bond formation. Also, by combination of advantages of GO as catalyst support and high catalytic activity of $[RuHCl(CO)(PPh_3)_3]$ in organic synthesis, the ability of graphene oxide supported catalyst, [Ru–H@TMSPT–GO], in the synthesis of symmetrical phenacyl benzoate derivatives under heterogeneous conditions is reported.

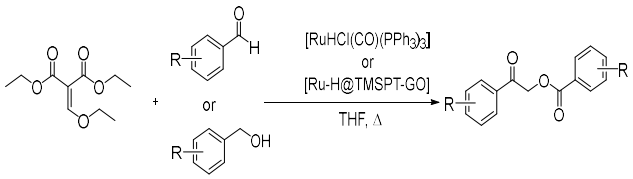

Scheme 1. Synthesis of symmetrical phenacyl benzoate derivatives catalyzd by homogeneous and heterogeneous ruthenium hydride catalysts

2. EXPERIMENTAL

Materials and methods

The chemicals were purchased from Fluka and Merck chemical companies. ^1H and ^{13}C NMR (400 and 100 MHz) spectra were recorded with a Bruker–Avance 400 spectrometer in $CDCl_3$. FT–IR spectra were recorded on a Jasco 6300D instrument in the range of 400–4000 cm^{-1}. Mass spectra were recorded on a Platform II spectrometer from Micromass; EI mode at 70 eV. Elemental analysis was performed on a LECO, CHNS–932 analyzer. Diffuse reflectance UV–Vis (DR UV–Vis) spectra were obtained on a JASCO, V–670 (190–2700 nm) spectrophotometer. The ICP analyses were performed on an ICP–Spectrociros CCD instrument. The TEM images were obtained using a Philips CM10 instrument. Scanning electron microscopy (SEM) images were taken by a Hitachi S–4800 field emission scanning electron microscope (FE–SEM). The Ru loading of the heterogeneous catalyst was determined using an inductively coupled plasma atomic emission spectrometer (ICP–AES). The products were purified by plate chromatography on silica gel (Merck KGaA, Silica Gel 60).

The $RuHCl(CO)(PPh_3)_3$ was prepared *via* methods reported in the literature.[47] Graphene oxide (GO) was oxidized from graphite powder by a modified Hummers method.[48]

Preparation of grapheme oxide functionalised with (3–mercaptopropyl)trimethoxysilane, TMSPT–GO

(3–Mercaptopropyl)trimethoxysilane (3 mL) in dry toluene (10 mL) was added dropwise to a suspension of GO (1 g) in dry toluene (50 mL). The mixture was refluxed with continuous stirring for 24 h under nitrogen atmosphere. After cooling the mixture, the black powder was filtered, washed with toluene and EtOH, and dried at 70 ºC under vacuum for 6 h.

Preparation of catalyst, [Ru–H@TMSPT–GO]

The TMSPT–GO (1 g) was dispersed in dry toluene (50 mL) by vigorous stirring and a solution of $[RuHCl(CO)(PPh_3)_3]$ (0.2 g) in dry toluene (10 mL) was added to this mixture. The mixture was refluxed for 24 h; the [Ru–H@TMSPT–GO] was filtered, washed with toluene to remove the excess reactants and dried under vacuum for 24 h.

Typical procedure for synthesis of symmetrical phenacyl benzoates

In a screw capped test tube, a mixture of freshly distilled aldehyde or benzyl alcohol (1.5 mmol), diethylethoxymethylenemalonate (DEMM) (216.2 mg, 1 mmol) and $[RuHCl(CO)(PPh_3)_3]$ (47.9 mg, 0.05 mmol) or [Ru–H@TMSPT–GO] (30 mg, 0.017 mmol) in THF (2 mL). The test tube was purged with argon and sealed. The reaction mixture was allowed to stir at 90 °C. In the case of homogeneous catalysis, the solvent was evaporated under reduced pressure. In the case of heterogeneous catalysis, the catalyst was filtered and washed with toluene. The solvent was evaporated under reduced pressure. The product was isolated by silica gel chromatography (petroleum ether/ethyl acetate = 80/1) and recrystallized from ethanol to give the corresponding phenacyl benzoate.

Phenacyl benzoate (3a). White solid; Mp 118-119 °C; ^1H NMR(400 MHz, $CDCl_3$): δ 5.59 (s, 2H), 7.45–7.62 (m, 6H), 7.97 (d, 2H, J = 7.6 Hz) 8.15 (d, 2H, J = 7.2 Hz); $^{13}C\{^1H\}$ NMR (100 MHz, $CDCl_3$): δ 192.1, 166.0, 134.3, 133.9, 133.1, 130.0, 128.8, 128.3, 127.8, 66.4; IR (KBr): ν_{max} 1722, 1692, 1585, 1453, 1410, 1368, 1275, 1218, 1119, 948, 756, 688 cm^{-1}; MS (EI, 70 eV): *m/z* 240, 118, 105, 77, 51, 27, 15.[32]

4–Nitrobenzoic acid–(4–nitro–phenacyl ester) (3b). Yellow solid; Mp 176–178 °C; ^1H NMR (400 MHz, $CDCl_3$): δ 5.40 (s, 2H), 7.45–7.48 (m, 4H), 8.17 (d, 2H, J = 8.8 Hz), 8.22 (d, 2H, J = 8.8 Hz); $^{13}C\{^1H\}$ NMR (100 MHz, $CDCl_3$): δ 190.7, 164.7, 137.3, 136.7, 136.6, 134.3, 134.0, 133.9, 133.4, 128.6, 128.4, 65.5; IR (KBr): ν_{max} 1729, 1654, 1525, 1463, 1371, 1350, 1273, 1097, 1013, 798, 709 cm^{-1}; MS (EI, 70 eV): *m/z* 163, 149, 121, 95, 97, 71, 69, 57, 43.

4–Chlorobenzoic acid–(4–chloro–phenacyl ester) (3c). White solid; Mp 119–120 °C; ^1H NMR (400 MHz, $CDCl_3$): δ 5.62 (s, 2H), 7.26–7.50 (m, 4H), 7.91 (d, 2H, J= 8.8 Hz), 8.11 (d, 2H, J = 8.8 Hz); $^{13}C\{^1H\}$ NMR (100 MHz, $CDCl_3$): δ 190.8, 164.4, 138.6, 133.3, 130.1, 130.0, 128.6, 127.8, 127.7, 127.3, 65.8; IR (KBr): ν_{max} 1725, 1701, 1590, 1486, 1425, 1396, 1368, 1283, 1226, 1127, 1090, 1009, 820, 758 cm^{-1}; MS (EI, 70 eV): *m/z* 152, 139, 111, 75, 50.[32]

4–Fluorobenzoic acid–(4–fluoro–phenacyl ester) (3d). White solid; Mp 117–120; ^1H NMR (400 MHz, $CDCl_3$): δ 5.24 (s, 2H), 6.97–7.10 (m, 4H), 7.33–7.35 (m, 2H), 7.98–8.00 (m, 2H); $^{13}C\{^1H\}$ NMR (100 MHz, $CDCl_3$): δ 197.7, 171.5, 166.3 (^1J = 171), 162.8 (^1J = 171.0 Hz), 132.2 (^3J = 9.0 Hz), 131.7, 130.3

(^4J = 8.0 Hz), 127.0, 115.6 (^2J = 22.0), 66.1; IR (KBr): ν_{max} 1736, 1685, 1604, 1510, 1430, 1373, 1294, 1233, 1158, 1124, 1029, 923, 855, 768 cm^{-1}; MS (EI, 70 eV): *m/z* 133, 123, 113, 94, 69, 54, 44.

2–Chlorobenzoic acid–(2–chloro–phenacyl ester) (3e). White solid; Mp 112–113 °C; ^{1}H NMR (400 MHz, $CDCl_3$): δ 5.41 (s, 2H), 7.39–7.45 (m, 3H), 7.35–7.38 (m, 3H), 7.47 (dd, 1H, *J* = 8.0 Hz), 7.81 (dd, 1H, *J* = 8.0 Hz); ^{13}C{^{1}H} NMR (100 MHz, $CDCl_3$): δ 195.9, 165.2, 133.3, 132.8, 131.6, 131.2, 130.2, 129.7, 129.6, 127.0, 126.6, 64.6; IR (KBr): ν_{max} 1712, 1634, 1588, 1436, 1409, 1382, 1311, 1251, 1162, 1114, 1090, 997, 752 cm^{-1}; MS (EI, 70 eV): *m/z* 152, 139, 124, 111, 99, 89, 84, 73, 62, 55, 49.

3–Bromobenzoic acid–(3–bromo–phenacyl ester) (3f). White solid; Mp 113–116 °C; ^{1}H NMR (400 MHz, $CDCl_3$): δ 5.24 (s, 2H), 7.16–7.18 (m, 2H), 7.20–7.39 (m, 2H), 7.39–7.42 (m, 1H), 7.60–7.63 (m, 1H), 7.1 (d, 1H, *J* = 0.6 Hz), 8.11 (d, 1H, *J* = 0.8 Hz); ^{13}C{^{1}H} NMR (100 MHz, $CDCl_3$): δ 191.6, 164.9, 137.9, 136.2, 132.7, 131.8, 131.3, 130.0, 128.3, 126.9, 122.7, 66.1; IR (KBr): ν_{max}1721, 1702, 1590, 1482, 1437, 1402, 1385, 1315, 1186, 1119, 1069, 1069, 952, 886, 753cm^{-1}; MS (EI, 70 eV): *m/z* 198, 183, 157, 155, 128, 107, 95, 7763, 50.

2,4–Dichlorobenzoic acid–(2,4–dichloro–phenacyl ester) (3g). White solid; Mp 101–103 °C; ^{1}H NMR (400 MHz, $CDCl_3$): δ 5.35 (s, 2H), 7.37–7.43 (m, 4H), 7.57–7.63 (m, 2H), 7.77 (d, 2H, *J* = 8.0 Hz); ^{13}C{^{1}H} NMR (100 MHz, $CDCl_3$): δ 191.2, 164.3, 138.7, 135.2, 134.7, 132.7, 131.7, 131.2, 129.6, 127.7, 127.1, 64.2; IR (KBr): ν_{max} 1725, 1699, 1588, 1556, 1476, 1374, 1292, 1246, 1152, 1132, 1103, 1048, 952, 904, 866, 824, 796, 767 cm^{-1}; MS (EI, 70 eV): *m/z* 203, 189, 186, 174, 145, 122, 109, 84, 73, 63, 55, 44.

4–Methylbenzoic acid–(4–methyl–phenacyl ester) (3h). White solid; Mp 141–142 °C; ^{1}H NMR (400 MHz, $CDCl_3$): δ 2.10 (s, 6H), 5.54 (s, 2H), 7.37–7.41 (m, 4H), 7.87 (d, 2H, *J* = 8.0 Hz), 8.04 (d, 2H, *J* = 8.0 Hz); ^{13}C{^{1}H} NMR (100 MHz, $CDCl_3$): δ 191.9, 166.1, 144.8, 144.1, 131.9, 130.0, 129.6, 129.2, 128.0, 126.7, 66.3, 21.8, 21.7; IR (KBr): ν_{max} 1719, 1690, 1595, 1442, 1406, 1362, 1274, 1223, 1172, 1107, 954, 801, 743 cm^{-1}; MS (EI, 70 eV): *m/z* 132, 119, 91, 65, 39.[32]

2–Thiophene–2–carboxylic acid–(thiophene–2–acylester) (3j). pale yellow solid; Mp 118–120°C; ^{1}H NMR (400 MHz, $CDCl_3$): δ 5.41 (s, 1H), 7.75 (d, 1H, *J* = 0.8), 7.73 (d, 1H, *J* = 1.2 Hz), 7.61 (d, 2H, *J* = 1.6 Hz), 7.58 (d, 2H, *J*= 1.6 Hz); ^{13}C{^{1}H} NMR (100 MHz, $CDCl_3$): δ 193.3, 159.8, 137.2, 133.8, 133.7, 128.7, 128.6, 128.5, 128.4, 63.91; IR (KBr): ν_{max} 1735, 1587, 1479, 1437, 1373, 1304, 1255, 1193, 1118, 1091, 1089, 1027, 998, 855, 747, 720 cm^{-1}; MS (EI, 70 eV): *m/z* 125, 111, 83, 58.

NMR study: Formation of a ruthenium enolate complex, [Ru{η3–(Et$_2$OC)$_2$C(H)O}Cl(CO)(PPh$_3$)$_2$] (I)

$RuHCl(CO)(PPh_3)_3$ (47.9 mg, 0.05 mmol) and $CDCl_3$ (2 mL) were placed in an NMR tube. The tube was purged with N_2, capped with a rubber septum, and heated at 90 °C for 10 min. After cooling to room temperature, EMME (216.2 mg, 1.0 mmol) was added. The resulting mixture was heated at 90 °C for 60 min. The formation of ruthenium enolate complex **I** was confirmed by ^{1}H and ^{13}C NMR measurements and recrystallized from $CHCl_3$ and hexane.

^{1}H NMR (400 MHz, $CDCl_3$) δ 1.19 (t, *J* = 7.2 Hz, 6H), 3.41 (t, ^3J(P–H) =1.4 Hz, 1H), 3.87 (q, *J* = 8.3 Hz, 4H), 7.39–7.44 (m, 12 H), 7.48–7.52 (m, 6H), 7.63–7.66 (m, 6H), 7.68–7.76 (m, 6H); ^{13}C{^{1}H} NMR (100 MHz, $CDCl_3$) δ 208.0 (t, ^2J (C–P) = 17.5), 163, 134.6 (t, ^3J (C–P) = 5.5), 134.0 (t, ^1J (C–P) = 20.5), 129.1, 127.4 (t, ^4J (C–P) = 4.5, 104.13, 89.3, 60.0, 10.2; ^{31}P NMR (160 MHz, $CDCl_3$) δ 29.2, 40.09; IR (KBr): ν_{max} 1918 cm^{-1}.

3. RESULTS AND DISCUSSION

Scheme 2 shows the preparation route for heterogeneous catalyst. As can be seen, first, the GO was functionalized with trimethoxysilylpropylthiol, TMSPT, as a linker. Next, $[RuHCl(CO)(PPh_3)_3]$ was reacted with GO functionalized TMSPT to produce the heterogeneous [Ru–H@TMSPT–GO] catalyst. The prepared catalyst was characterized by different analytical techniques to confirm the attachment of ruthenium catalyst on the GO nanosheets. The sulfur content of the support was 14.1%. According to this value, the amount of S which is available for attachment of $[RuHCl(CO)(PPh_3)_3]$ is about 2.2 mmol/g. The amount of Ru in the supported catalyst, determined by ICP, was about 0.55% (0.055 mmol/g).

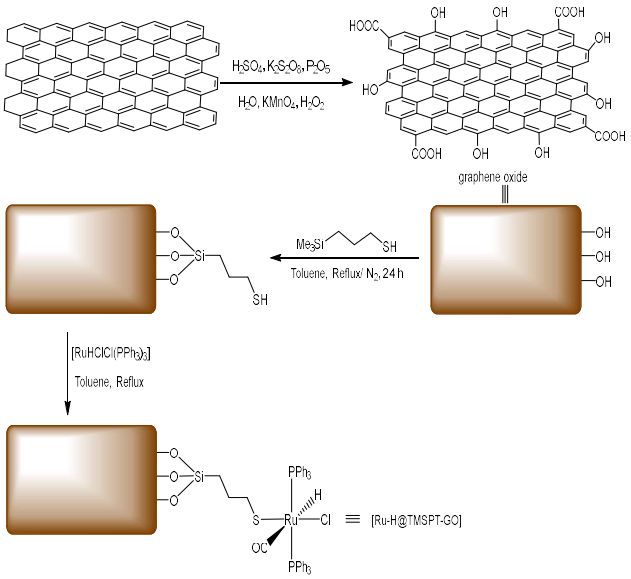

Scheme 2. Preparation route for [Ru–H@TMSPT–GO]

The FT–IR spectra of GO, GO–TMSPT and [Ru–H@TMSPT–GO] are shown in Fig. 1. Compared to the FT–IR spectrum of GO (Fig. 1A), the appearance of bands at 1097 (Si–O–Si), 1019 (Si–O–C) 2923 and 2889 (aliphatic C–H) in the FT–IR spectrum of TMSPT (Fig. 1B) is a good confirmation for attachment of TMSPT to the surface of GO. The FT–IR spectra of homogeneous $[RuHCl(CO)(PPh_3)_3]$ showed characteristic bands at 2013 cm^{-1}(Ru–H) and 1925 cm^{-1} (C=O). Upon immobilization, these two bands shifted to 2059, and 1948 cm^{-1}, respectively (Figure 1). The presence of these vibrational bands in the FT–IR spectrum of heterogeneous catalyst confirmed the successful attachment of $[RuHCl(CO)(PPh_3)_3]$ on the GO.

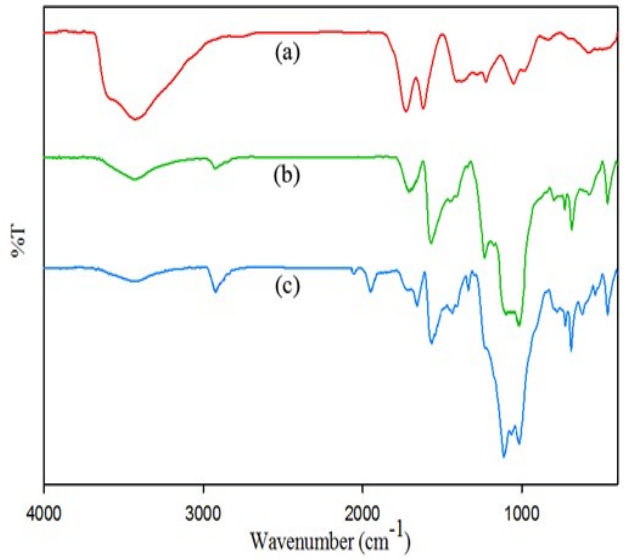

Figure 1. FT–IR spectra of (a) GO, (b) GO–TMSPT and (c) [Ru–H@TMSPT–GO].

The UV–vis spectra of TMSPT–GO and [Ru–H@TMSPT–GO] in the diffuse reflectance mode are shown in Figure 2. The ruthenium hydride complex, $RuHCl(CO)(PPh_3)_3$, has a characteristic absorption peak at 329 nm.[45] The TMSPT–GO exhibits an absorption peak at 272 nm (Fig. 2A), whereas the [Ru–H@TMSPT–GO] showed two peaks at 271 nm and 334 nm (Fig. 2B). The former is attributed to the support and the latter is corresponded to the Ru complex with a red shift in comparison with non–supported complex.

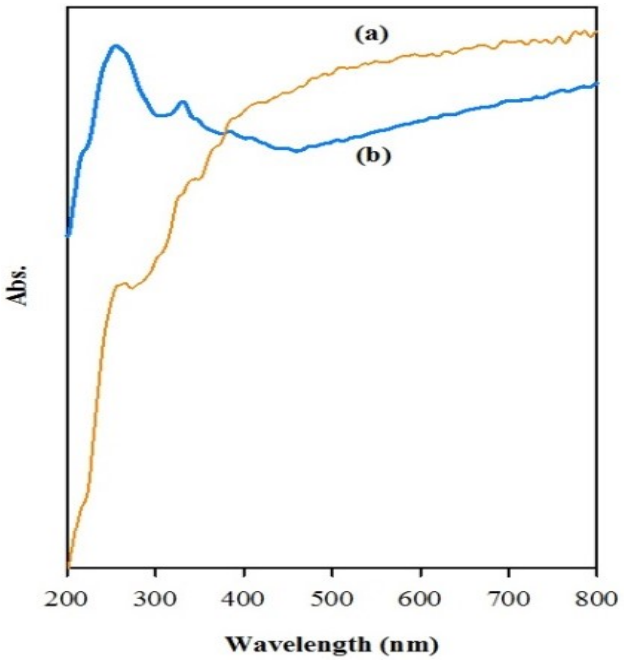

Figure 2. The UV–vis spectra of (a) TMSPT–GO and (b) [Ru–H@TMSPT–GO].

Figure 3 shows the Raman spectra of GO and [Ru–H@TMSPT–GO]. The Raman spectrum of GO (Figure 3a), two characteristics bands i.e. the D band (1368 cm^{-1}) and the G band (1610 cm^{-1}) have about equal intensity. The integral intensity ratio of D and G bands (I_D/I_G) was found to be 1.0 which indicates a large number of defects in GO in the form of epoxide and other oxygen containing functionalities. Compared to GO, the D and G bands in the case of [Ru–H@TMSPT–GO] were appeared at 1362 and 1362 cm^{-1}, respectively (Figure 3b). Further the I_D/I_G value decreased to 0.70, indicating the successful attachment of ruthenium hydride complex to the GO support.[49]

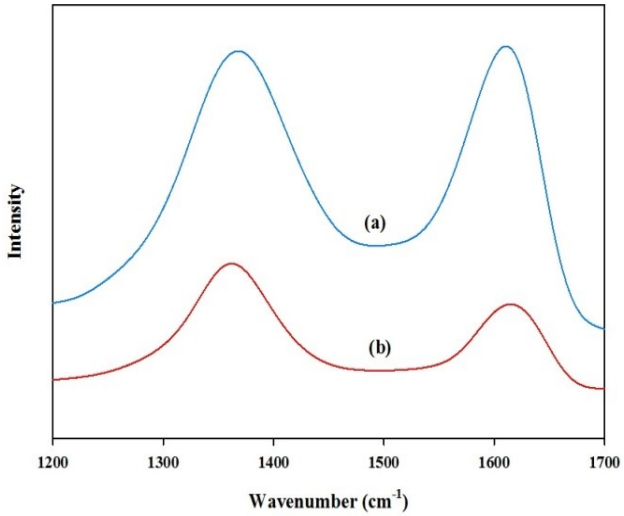

Figure 3. Raman spectra of (a) GO and (b) [Ru–H@TMSPT–GO].

The FE–SEM images of GO and [Ru–H@TMSPT–GO] are shown in Figure 4. It can be seen that GO has a layered and wrinkled structure (Figure 4A). Compared to GO nanosheets, the FE–SEM image of [Ru–H@TMSPT–GO] (Figure 4B) exhibited an agglomerated layered structure incorporating the ruthenium complex moieties between the sheets.

Energy dispersive (X–Ray spectroscopy) analyses of GO and [Ru–H@TMSPT–GO] were shown in (Figure 5). As can be seen, in the EDX spectrum of GO (Figure 5A), the major elements are carbon and oxygen while after attachment of ruthenium hydride catalyst on the TMSPT–GO, the presence of the Ru, S and Si peaks originates from TMSPT and $[RuHCl(CO)(PPh_3)_3]$ (Figure 5B) is a good indication for attachment of ruthenium catalyst on GO nanosheets. The corresponding elemental mapping of the heterogeneous catalyst was also performed to understand the distribution of the Ru on TMSPT–GO. As can be seen, Ru has a uniform distribution in the catalyst texture which showed successful immobilization of the catalyst on TMSPT–GO (Figure 6).

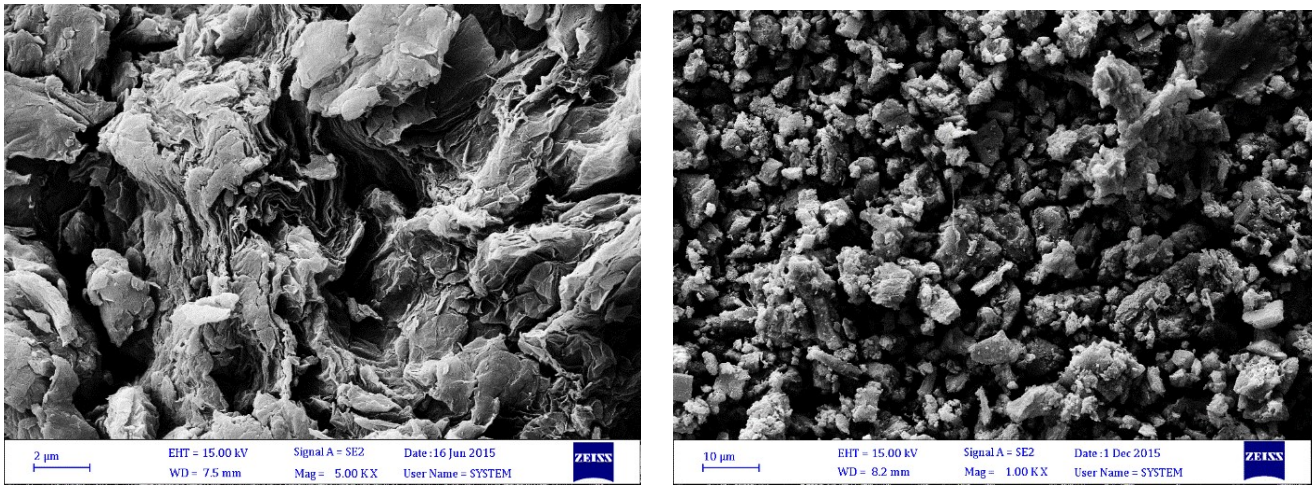

(A) **(B)**

Figure 4. FE–SEM images of (A) GO and (B) [Ru–H@TMSPT–GO].

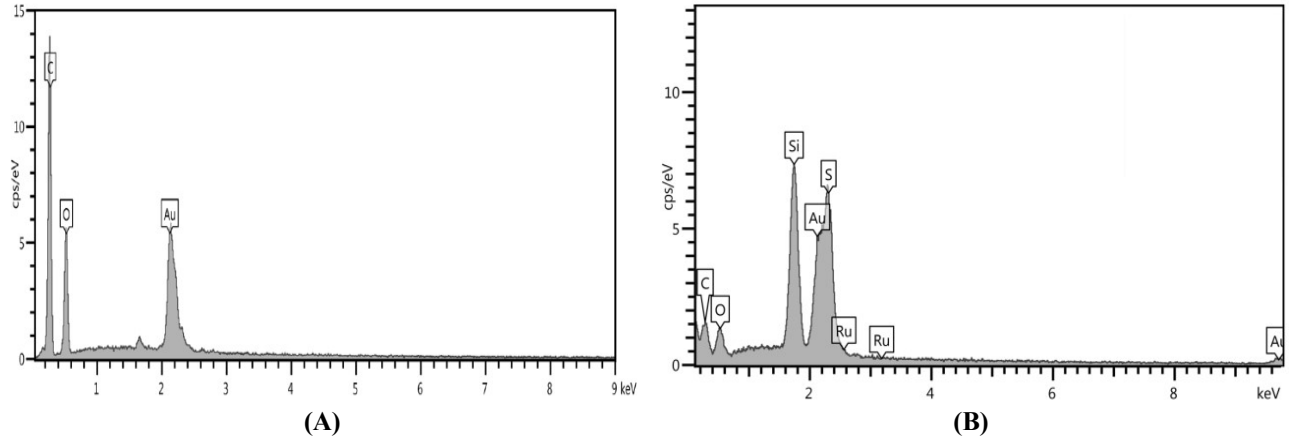

(A) **(B)**

Figure 5. EDX spectrum of (A) GO and (B) [Ru–H@TMSPT–GO].

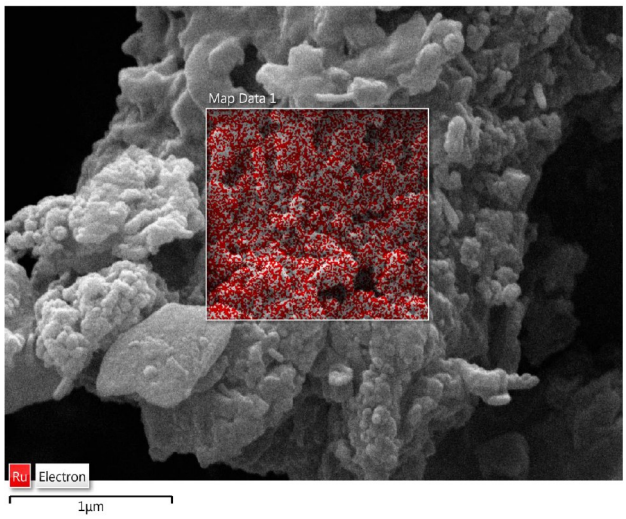

Figure 6. Mapping image of [Ru–H@TMSPT–GO].

The catalyst texture was also studied by transmission electron microscopy (TEM). It is well known that the TEM image of GO shows transparent stacked sheets having well defined edges. The TEM image of [Ru–H@TMSPT–GO] (Figure 7) shows evenly distributed dark spots, which are probably due to the attachment of the Ru complex on the GO support.

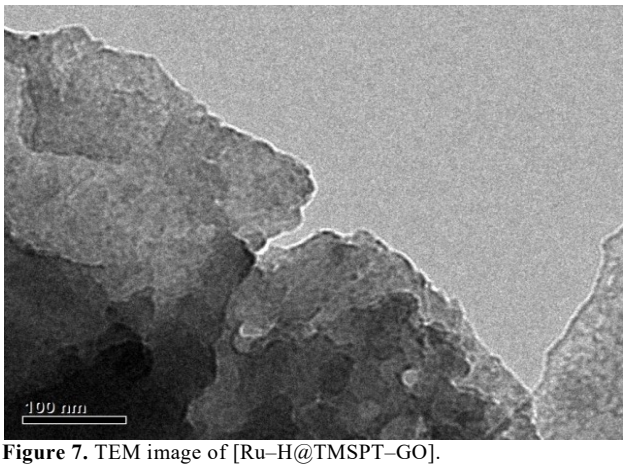

Figure 7. TEM image of [Ru–H@TMSPT–GO].

After preparation and characterization of haterogeneous catalyst, The catalytic activity of homogeneous and heterogeneous counterpart was investigated in the synthesis of phenacyl benzoates. Initial studies were focused on the coupling of DEMM (**1**) with benzaldehyde (**2a**) as model reaction for the optimization of reaction conditions (Table 1). First, the kind of Ru catalyst was optimized in the model reaction. In this manner, the catalytic activity of $[RuHCl(CO)(PPh_3)_3]$, $[RuH_2(CO)(PPh_3)_2]$ and $[Ru(O_2CCF_3)(CO)(PPh_3)_2]$ was investigated. The results revealed that $[RuHCl(CO)(PPh_3)_3]$ is much more efficient than $[RuH_2(CO)(PPh_3)_2]$ and $[Ru(O_2CCF_3)(CO)(PPh_3)_2]$ (entries 1–3).

Investigation of the catalyst amount showed that the highest yield was obtained using 5 mol% of catalyst. Then, the effect of different solvents was studied in the model reaction. As can be seen the highest yield was obtained using THF as reaction media (entries 3, 6 and 7). The effect of temperature was also investigated and the results showed that increasing the temperature more than 90 °C did not affect the yield but reducing it to 70 °C resulted in lower yield (entries 8 and 9). When the model reaction was carried out in the absence of catalyst, no appreciable amount of the corresponding phenacyl was observed (entry 10).

To explore the scope and generality of this process, different aldehydes (**2**) were reacted with DEMM (**1**) under the optimized conditions (Table 2). The reaction of DEMM with benzaldehdes bearing electron–withdrawing groups proceeds more efficiently (entries 2–7) than benzaldehydes constitute electron–donating substituent such as 4–methylbenzaldehyde(entry 8).

Table 1. Optimization of reaction conditions in the reaction of DEMM (**1**) with benzaldehyde (**2a**)

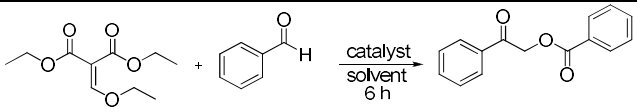

1 **2a** **3a**

Row	Catalyst	Cat. (mol%)	Solv.	T (°C)	Yield (%)[b]
1	$[RuH_2(CO)(PPh_3)_2]$	5	THF	90	35
2	$[Ru(O_2CCF_3)_2(CO)(PPh_3)_2]$	5	THF	90	8
3	$[RuHCl(CO)(PPh_3)_3]$	5	THF	90	79
4	$[RuHCl(CO)(PPh_3)_3]$	3	THF	90	56
5	$[RuHCl(CO)(PPh_3)_3]$	7	THF	90	79
6	$[RuHCl(CO)(PPh_3)_3]$	5	Benzene	80	0
7	$[RuHCl(CO)(PPh_3)_3]$	5	$C_2H_4Cl_2$	90	10
8	$[RuHCl(CO)(PPh_3)_3]$	5	THF	70	20
9	$[RuHCl(CO)(PPh_3)_3]$	5	THF	110	79
10	[Ru–H@TMSPT–GO]	0.17 (30 mg)	THF	90	78
11	[Ru–H@TMSPT–GO]	0.27 (50 mg)	THF	90	78
12	[Ru–H@TMSPT–GO]	0.11 (20 mg)	THF	90	46
13	No catalyst	–	THF	90	5>

[a]Reaction conditions: **1** (1 mmol), **2a** (1.5 mmol), catalyst and solvent (2 mL) for 6 h in a screw capped test tube. [b]The yields refer to pure isolated material.

Table 2. Ruthenium–Hydride Catalyzed Coupling of DEMM (**1**) with Aldehydes (**2**)[a]

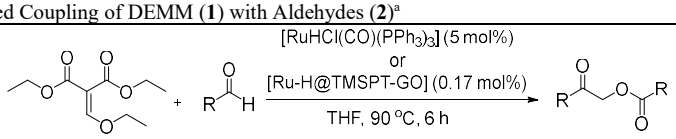

1 (1 mmol) **2** (1.5 mmol) **3**

Row	R		Product (3)	Yield (%)[b]	
				[RuHCl(CO)(PPh3)3]	[Ru–H@TMSPT–GO]
1	C_6H_5	**2a**	**3a**	79	78
2	4–$NO_2C_6H_4$	**2b**	**3b**	96	94
3	4–ClC_6H_4	**2c**	**3c**	85	86
4	4–FC_6H_4	**2d**	**3d**	87	85
5	2–ClC_6H_4	**2e**	**3e**	84	85
6	3–BrC_6H_4	**2f**	**3f**	90	91
7	2,4–$Cl_2C_6H_3$	**2g**	**3g**	91	90
8	4–$CH_3C_6H_4$	**2h**	**3h**	75	72
9	4–$CH_3OC_6H_4$	**2i**	**3i**	0	0
10	3–Thienyl	**2j**	**3j**	64	68
11	$CH_3CH_2CH_2$	**2k**	**3k**	0	0

[a]Reacion conditions: DEMM (1 mmol), aldehyde (1.5 mmol), catalyst and THF (2 mL) for 6 h in a screw capped test tube. [b]The yields refer to pure isolated material.

But, benzaldehydesbearing strong electron–donating substituent such as 4–methoxybenzaldehyde did not react and remained intact in the reaction mixture (entry 9). When, thionyl–3–carbaldehyde (**2j**) was reacted with DEMM, the corresponding phenacyl was produced in 64% isolated yield (entry 10). But in the reaction of butyraldehyde (**2k**) with DEMM, no product was observed and the initial aldehyde was recovered from reaction mixture (entry 11). It seems that aldehydes bearing electron–withdrawing substituents were more reactive than aldehydes with electron–donating groups.

Under the same reaction conditions used for the reaction of aldehydes with DEMM, we investigated the reaction of alcohols with DEMM (Table 3). The DEMM reacted with substituted benzyl alcohols in the presence of [$RuHCl(CO)(PPh_3)_3$] and gave the desired products in good to excellent yields. The same results were also obtained in the case of alcohols and the alcohols bearing electron–withdrawing substituents were more reactive than alcohols containing electron–donating groups. The reaction time in the case of aldehydes was 6 h while in tha case of alcohols was 8 h. In the later, the alcohols first oxidize to aldehydes and then react with DEMM.

The main problem associated with homogeneous catalyst is that this catalyst is not recoverable and reusable. To solve this problem, we decided to investigate the ability of heterogeneous catalyst in the synthesis of phenacyl derivatives. First, the amount of catalyst was optimized in the model reaction. Among the different catalyst amounts, 0.17 mol% (30 mg) of the catalyst was chosen as the optimized amount (Table 1, entries 10–12). As described for the homogeneous catalytic system, the THF and 90 ºC were selected as solvent and reaction temperature.

Under the optimized reaction conditions (0.17 mol% of catalyst in THF at 90 ºC), different aldehydes were reacted with DEMM and the corresponding phenacyl benzoates were produced in good to excellent yields (Table 2). As same as homogeneous conditions, 4–methoxybenzaldehyde and butyraldehyde were inactive in this catalytic system.

Under the heterogeneous conditions, alcohols were also reacted with DEMM and the corresponding phenacyl benzoates were produced in good to excellent isolated yields (Table 3). The higher catalytic activity of [Ru–H@TMSPT–GO] compared to [$RuHCl(CO)(PPh_3)_3$] can be attributed to the dispersion of catalytic species on the grapheme oxide nanosheets. The isolation of the catalytic active sites makes them more accessible for substrates.

The reaction mechanism is not clear at present but according to the C–O bond cleavage previously reported in the reaction of allyl esters in the presence of ruthenium hydride, affording propene and methane,[50] a mechanism for the synthesis of symmetrical phenacyl benzoate derivatives is proposed (Scheme 3). First, the reaction of DEMM (**2**) with ruthenium hydride catalyst, [$RuHCl(CO)(PPh_3)_3$], was investigated in the absence of aldehyde. Under these conditions, the C–O bond cleavage was occurred[50] and the ruthenium enolate **I** along with ethane were produced, which further confirmed by ^{1}H NMR spectroscopy. Then, the complex **I** reacts with benzaldehyde **2a** to give the complex **II** which can be transformed to **III** and/or **IV**. Finally, *β*–ruthenium complex **IV** reacts with aldehyde **2a** to givethe complex **V** which upon elimination of diethyl malonate, affords the desired product **3a**. These observations are in accordance to the previous reports.[19,51]

The reusability of the heterogeneous catalyst was also investigated in the reaction of DEMM (**1**) with 4–nitrobenzaldehyde (**2a**). In this mannner, after each catalytic cycle, the catalyst was filtered, washed with THF and diethyl ether, and dried. The reused catalyst was used in the reaction of fresh DEMM with benzaldehyde. The results showed that the catalyst was reused four consecutive times without a significant

Table 3. Ruthenium–Hydride Catalyzed Coupling of DEMM (**1**) with Benzyl Alcohols (**4**)[a]

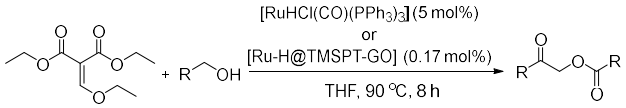

1 (1 mmol) **4** (1.5 mmol) **3**

Row	R		Product (3)	Yield (%)[b]	
				[$RuHCl(CO)(PPh_3)_3$]	[Ru–H@TMSPT–GO]
1	C_6H_5	**4a**	**3a**	76	77
2	4–$NO_2C_6H_4$	**4b**	**3b**	93	91
3	4–ClC_6H_4	**4c**	**3c**	81	83
4	4–FC_6H_4	**4d**	**3d**	83	81
5	2–ClC_6H_4	**4e**	**3e**	82	80
6	3–BrC_6H_4	**4f**	**3f**	92	91
7	2,4–$Cl_2C_6H_3$	**4g**	**3g**	90	89
8	4–$CH_3C_6H_4$	**4h**	**3h**	74	75

[a]Reacion conditions: DEMM (1 mmol), alcohol (1.5 mmol), catalyst and THF (2 mL) for 8 h in a screw capped test tube. [b]The yields refer to pure isolated material.

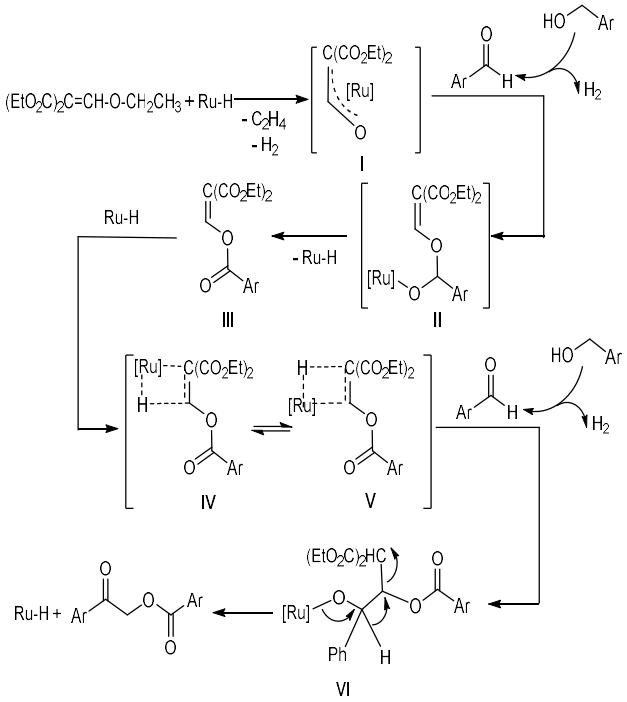

Scheme 3. Proposed mechanism

loss of its activity (Figure 8). The amount of catalyst leached was measured by ICP. The results showed that about 4% of the initial Ru content was leached after the first run. No Ru was detected in the filtrates in next three runs. The hot–filtration test was also performed. In this manner, the catalyst was filtered off in the modal reaction after 3 hours (29% conversion) and the filtrate was then stirred at 90 °C. The results showed that the reaction progress was only 3%. …..

The nature of recovered catalyst was studied by FT–IR spectroscopy. The presence of the bands at 2052 and 1946 cm^{-1} in the FT–IR spectrum of the recovered catalyst (Figure 9) confirmed that the ruthenium complex has retained its initial structure during the catalytic experiments.

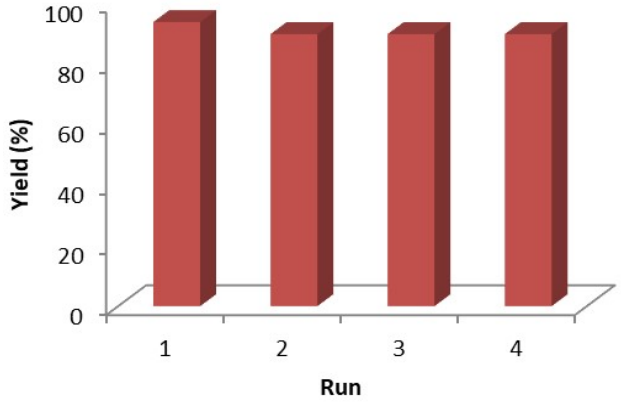

Figure 8. Reusability of the catalyst.

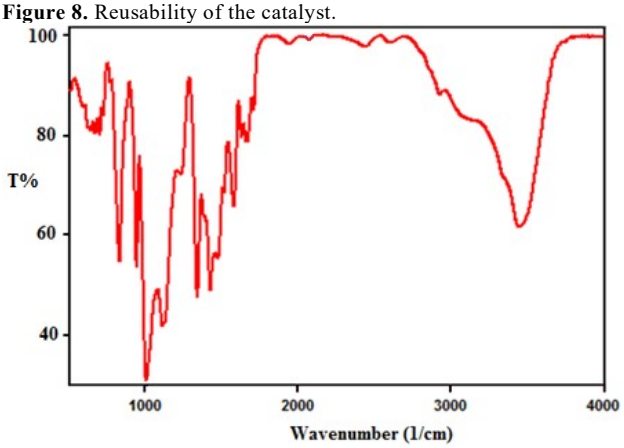

Figure 9. The FT-IR of recovered catalyst.

4. CONCLUSIONS

In summary, ruthenium–catalyzed transfer hydrogenation of DEMM in the presence of different aldehydes or alcohols furnished phenacyl benzoate derivatives which are a fundamental class of organic compounds in organic synthesis. We have also found as further C–C bond–forming catalyzed by ruthenium, construction of sp^2–C–O bond is also too. Furthermore, this process represents a way for extension of utilization of ruthenium hydride catalysts in organic synthesis. On the other hand, the heterogeneous catalyst was also applied in this catalytic system and good to excellent yield was obtained. Low catalyst amount, simple work–up and catalyst reusabilty are the advantages of heterogeneous system.

CONFLICTS OF INTEREST

The authors declare that they have no known competing financial interests or personal relationships that could have appeared to influence the work reported in this paper.

ACKNOWLEDGMENTS

The finalcial support of this work by the Research Council of The Uinversity of Isfahan is acknowledged.

AUTHOR INFORMATION

Corresponding Author

Majid Moghadam: Email: moghadamm@sci.ui.ac.ir, ***ORCID***: 0000-0001-8984-1225

Author(s)

Shahram Tangestaninejad, Valiollah Mirkhani, Iraj Mohammadpoor–Baltork, Behjat Barati, Moloud Ghafouri

REFERENCES

1. C. Bee, S. B. Han, A. Hassan, H. Iida, M. J.

Krische, *J. Am. Chem. Soc.* **2008**, *130,* 2746.
2. X. Cui, K. Burgess, *Chem. Rev.* **2005**, *105*, 3272.
3. K. I. Fujita, C. Asai, T. Yamaquchi, F. Hanasaka, R. Yamaguchi, *Org. Lett.* **2005**, *7*, 4017.
4. K. Källström, I. Munslow, P. G. Anderssen, *Chem. Eur. J.* **2006**, *12*, 3194.
5. C. Löfberg, R. Grigg, M. A. Whittaker, A. Keep, A. Derrick, *J. Org. Chem.* **2006**, *71*, 8023.
6. M. Y. Ngai, A. Barchuk, M. J. Krische, *J. Am. Chem. Soc.* **2007**, *129*, 12644.
7. J. F. Bower, E. Skucas, R. L. Patman, M. J. Krische. *J. Am. Chem. Soc.* **2007**, *129*, 15134.
8. M. Y. Ngai, W. Skucas, M. J. Krische, *Org. Lett.* **2008**, *10*, 2705.
9. F. Shibahara, J. F. Bower, M. J. Krische, *J. Am. Chem. Soc.* **2008**, *130*, 6338.
10. R. L. Patman, V. M. Williams, J. F. Bower, M. J. Krische, *Angew. Chem., Int. Ed.* **2008**, *47,* 5220.
11. S. Omura, T. Fukuyama, J. Horiguchi, Y. Murakami, I. Ryu, *J. Am. Chem. Soc.* **2008**, *130*, 14094.
12. R. L. Patman, M. R. Chaulagain, V. M. Williams, M. J. Krische, *J. Am. Chem. Soc.* **2009**, *131*, 2066.
13. E. Skucas, J. R. Zbieg, M. J. Krische, *J. Am. Chem. Soc.* **2009**, *131*, 5054.
14. G. Guillena, D. J. Ramón, M. Yus, *Angew. Chem. Int. Ed.* **2007**, *119*, 2410.
15. M. H. S. A. Hamid, P. A. Slatford, J. M. J. Williams, *Adv. Synth. Catal.* **2007**, *349*, 1555.
16. L. Shi, Y. Q. Tu, M. Wang, F. M. Zhang, C. A. Fan, Y. M. Zhao, W. J. Xia, *J. Am. Chem. Soc.* **2005**, *127*, 10836.
17. E. Skucas, M. Y. Ngai, V. Komanduri, M. J. Krische, *Acc. Chem. Res.* **2007**, *40*, 1394.
18. A. Barchuk, M. Y. Ngai, M. J. Krische, *J. Am. Chem. Soc.* **2007**, *129,* 8432.
19. T. Fukuyama, T. Doi, S. Minamino, S. Ommura, I. Ryu, *Angew. Chem. Int. Ed.* **2007**, *46*, 5559.
20. E. Skucas, J. F. Bower, M. J. Krische, *J. Am. Chem. Soc.* **2007**, *129*, 12678.
21. F. Shibahara, J. F. Bower, M. J. Krische, *J. Am. Chem. Soc.* **2008**, *130*, 14120.
22. J. F. Bower, R. L. Patman, M. J. Krische, *Org. Lett.* **2008**, *10*, 1033.
23. J. R. Kong, M. Y. Ngai, M. J. Krische, *J. Am. Chem. Soc.* **2006**, *128*, 718.
24. J. Peng, C. Zong, M. Ye, T. Chen, D. Gao, Y. Wang, C. Chen, *Org. Biomol. Chem.* **2011**, *9*, 1225.
25. D. G. Chan, D. J. Winternheimer, C. A. Merlic, *Org. Lett.* **2011**, *13*, 2778.
26. J. F. Hartwig, *Nature* **2008**, *455,* 314.
27. S. S. Gandhi, K. L. Bell, M. S. Gibson, *Tetrahedron* **1995**, *51*, 13301.
28. W. Huang, J. Pian, B. Chen, W. Pei, X. Ye, *Tetrahedron* **1996**, *52*, 10131.
29. R. Ruzicka, M. Zabadal, P. Klan, *Synth. Commun.* **2002**, *32*, 2581.
30. J. Literak, A. Dostálová, P. Klan, *J. Org. Chem.* **2006**, *71*, 713.
31. W. L. Judefind, E. E. Reid, *J. Am. Chem. Soc.* **1920**, *42*, 1043.
32. J. L. Wang, J. Q. Wang, L. N. He, X. Y. Dou, F. Wu, *Green Chem*. **2008**, *10*, 1218.
33. A. B. Bourlions, D. Gournis, D. Petridis, T. Szabo, A. Szeri, I. Dekany, *Langmuir* **2003**, *19*, 6050.
34. A. K. Geim, *Science* **2009**, *324*, 1530.
35. Y. B. Zhang, Y. W. Tan, H. L. Stormer, P. Kim, *Nature* **2005**, *438*, 201.
36. D. S. Su, S. Perathoner, G. Centi, *Chem. Rev.* **2013**, *113*, 5782.
37. D. R. Dreyer, S. Park, C. W. Bielawski, R. S. Ruoff, *Chem. Soc. Rev.* **2010**, *39*, 228.
38. O. C. Compton, S. T. Nguyen, *Small* **2010**, *6*, 711.
39. G. M. Scheuermann, L. Rumi, P. Steurer, W. Bannwarth, R. Mulhaupt, *J. Am. Chem. Soc.* **2009**, *131*, 8262.
40. H. P. Mungse, S. Verma, N. Kumar, B. Sain, O. P. Khatri, *J. Mater. Chem.* **2012**, *22*, 5427.
41. H. Su, Z. Li, Q. Huo, J. Guan, Q. Kan, *RSC Adv.* **2014**, *4*, 9990.
42. M. A. Nasseri, A. Allahresani, H. Raissi, *RSC Adv.* **2014**, *4*, 26087.
43. B. Barati, M. Moghadam, A. Rahmati, S. Tangestaninejad, V. Mirkhani, I. Mohammadpoor–Baltork, *Synlett* **2013**, *24*, 90.
44. B. Barati, M. Moghadam, A. Rahmati, V. Mirkhani, S. Tangestaninejad, I. Mohammadpoor–Baltork, *Inorg. Chem. Commun.* **2013**, *29*, 114.
45. B. Barati, M. Moghadam, A. Rahmati, V. Mirkhani, S. Tangestaninejad, I. Mohammadpoor–Baltork, *J. Organomet. Chem.* **2013**, *724*, 32.
46. A. Daneshvar, M. Moghadam, S. Tangestaninejad, V. Mirkhani, I. Mohammadpoor–Baltork, A. Khalili, *Organometallics* **2016**, *35*, 1747.
47. N. Ahmad, J. J. Levison, S. D. Robinson, M. F. Uttley, E. R. Wonchoba, G. W. Parshall, *Inorg. Synth.* **1974**, *15*, 45.
48. W. S. Hummers, R. E. Offeman, *J. Am. Chem. Soc.* **1957**, *80*, 1339.
49. S. Kumar, P. Kumar, S. L. Jain, *J. Mater. Chem. A* **2014**, *2*, 18861.
50. R. S. Srivastava, *Appl. Organomet. Chem.* **1993**, *7*, 607.
51. C. Podesva, G. Kohana, K. Vagi, *Can. J. Chem.* **1969**, *47*, 489.